

AD-A066 174

NAVAL RESEARCH LAB WASHINGTON D C
THEORY OF SOLID STATE CYCLOTRON MASER.(U)
JAN 79 A K GANGULY, K R CHU

F/G 20/5

UNCLASSIFIED

NRL-MR-3912

SBIE-AD-E000 274

NL

| OF |

AD
A066 174



END
DATE
FILMED

'5--79'
DDC

(13) **LEVEL III**
NW

ADE 000 274

NRL Memorandum Report 3912

Theory of Solid State Cyclotron Maser

A. K. GANGULY

*Microwave Technology Branch
Electronics Technology Division*

and

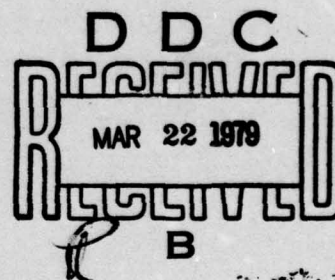
K.R. CHU

*Electron Beam Applications Branch
Plasma Physics Division*

ADA066174

DDC FILE COPY

January 31, 1979



79 02 08 003

NAVAL RESEARCH LABORATORY
Washington, D.C.

Approved for public release; distribution unlimited.

61153N

SECURITY CLASSIFICATION OF THIS PAGE (When Data Entered)

REPORT DOCUMENTATION PAGE		READ INSTRUCTIONS BEFORE COMPLETING FORM
1. REPORT NUMBER NRL Memorandum Report 3912	2. GOVT ACCESSION NO.	3. RECIPIENT'S CATALOG NUMBER
4. TITLE (and Subtitle) THEORY OF SOLID STATE CYCLOTRON MASER	5. TYPE OF REPORT & PERIOD COVERED Interim report on a continuing NRL problem	
7. AUTHOR(s) A. K. Ganguly and K. R. Chu	6. PERFORMING ORG. REPORT NUMBER	
9. PERFORMING ORGANIZATION NAME AND ADDRESS Naval Research Laboratory Washington, DC 20375	8. CONTRACT OR GRANT NUMBER(s)	
11. CONTROLLING OFFICE NAME AND ADDRESS	10. PROGRAM ELEMENT, PROJECT, TASK AREA & WORK UNIT NUMBERS NRL Problem R18-16 Subtask RR0110941	
14. MONITORING AGENCY NAME & ADDRESS (if different from Controlling Office) 35p.	12. REPORT DATE January 26, 1979	
	13. NUMBER OF PAGES 34	
	15. SECURITY CLASS. (of this report) UNCLASSIFIED	
16. DISTRIBUTION STATEMENT (of this Report) Approved for public release; distribution unlimited.		
17. DISTRIBUTION STATEMENT (of the abstract included in Block 20, if different from Report) AD-E000 274		
18. SUPPLEMENTARY NOTES		
19. KEY WORDS (Continue on reverse side if necessary and identify by block number) Solid state Cyclotron maser Electron beam Electromagnetic waves		
20. ABSTRACT (Continue on reverse side if necessary and identify by block number) A theory is developed for the cyclotron maser interaction between an electron beam and the electromagnetic waves in a cavity formed with a semiconductor having nonparabolic energy bands. The interaction originates from the dependence of the effective mass of the electron (hence cyclotron frequency) on its velocity due to nonparabolic energy-momentum relation. This mechanism is very similar to that for the cyclotron maser radiation in vacuum tubes where the relativistic variation of mass with velocity is utilized. The linear response of the electron beam		


DD FORM 1473
1 JAN 73

EDITION OF 1 NOV 65 IS OBSOLETE
S/N 0102-014-6601

251 950
SECURITY CLASSIFICATION OF THIS PAGE (When Data Entered)
79 02 08 003

20. Abstract (Continued)

to the cavity fields are obtained from Vlasov equation and the Maxwell's equations while collisions are treated with an approximate model. Analytical expressions for the beam-wave coupling coefficient, beam energy loss and the threshold power are derived for the fundamental and higher cyclotron harmonics. The dependence of these quantities on the various parameters such as cavity length, beam position, beam energy, magnetic field, etc. are discussed.



CONTENTS

I. INTRODUCTION	1
II. MODEL AND FORMULATION	5
III. BEAM POWER GAIN AND THRESHOLD POWER	11
IV. NUMERICAL RESULTS AND DISCUSSION	17
V. CONCLUSION	20
APPENDIX A	21
APPENDIX B	23
REFERENCES	25

ACCESSION for		
NTIS	White Section	<input checked="" type="checkbox"/>
DDC	Buff Section	<input type="checkbox"/>
UNANNOUNCED		<input type="checkbox"/>
JUSTIFICATION _____		
BY _____		
DISTRIBUTION/AVAILABILITY CODES		
Dist.	AVAIL.	and/or SPECIAL
A		

THEORY OF SOLID STATE CYCLOTRON MASER

I. INTRODUCTION

The cyclotron maser radiation^{1,2} in an electron beam in vacuum originates from the relativistic variation of electron mass (hence the cyclotron frequency) with velocity. In semiconductors such as InSb, the effective mass of the electrons depend on velocity due to the nonparabolic nature of the energy bands. This property can be utilized to make a solid state cyclotron maser³ (CM) in such semiconductors. The maser will operate in the submillimeter range and provide a low-power source of radiation in this frequency range.

As shown by Kane,⁴ the energy (W_b) of electrons in the conduction band of InSb is related to momentum (\vec{p}) by

$$W_b = \left[\left\{ E_g^2 + \frac{2E_g p^2}{m_o^*} \right\}^{1/2} - E_g \right] / 2$$

where m_o^* is the effective mass of the electrons at the bottom of the conduction band and E_g the band gap. From this equation and the relation⁵ $\vec{v} = \nabla_{\vec{p}} W_b$, it follows that $\vec{v} = \vec{p} / m_o^* (1 + p^2 / m_o^{*2} v_g^2)^{1/2} \equiv \vec{p} / m^*$, where the parameter m^* is

$$m^* = m_o^* \left[1 + \frac{p^2}{m_o^{*2} v_g^2} \right]^{1/2} = m_o^* \left[1 - v^2 / v_g^2 \right]^{-1/2} \quad (1)$$

and $v_g = \left[E_g / 2 m_o^* \right]^{1/2}$. In InSb $E_g \approx 0.24$ eV, $v_g \approx 1.30 \times 10^6$ m/sec and $m_o^* \approx .014 m_e$ where m_e is the free electron mass. Because of small values of m_o^* the solid state cyclotron maser can operate in the submillimeter frequency range with relatively weak magnetic fields of the order of several kilogauss.

If a thin InSb sample at 77°K is placed in a magnetic field B_o and electrons are injected in the conduction band at an angle to the magnetic field, the electrons will move in helical trajectories. Initially, the phases of the electrons in the cyclotron orbits are random and no radiation is emitted. But phase bunching can occur due to the dependence of cyclotron

Note: Manuscript submitted November 16, 1978.

frequency $\Omega = e B_0 / m^*$ on the electron energy. The electrons that are decelerated in the wave electric field rotate faster and accumulate phase lead while the electrons that are accelerated rotate slower and lag in phase. This results in phase bunching and the electrons radiate coherently at frequency $\omega = s\Omega$ where s is an integer. This mechanism of maser radiation is different from the optically pumped "cyclotron maser" proposed earlier.^{6,7}

Theoretical calculations for cyclotron maser in vacuum have been given for two different configurations, (1) the waveguide structure⁸ and (2) the cavity structure.⁹ In the first configuration, the electromagnetic wave grows as the result of an instability driven by the electron beam. It corresponds to travelling wave amplification in waveguide structures. In the second model, the electron beam interacts with the constant amplitude standing wave of a cavity structure. It corresponds to beam sustained oscillations in a finite Q cavity. Recently a theoretical treatment of cyclotron maser in solids was given by Kalmykov et al.³ for the waveguide structure. In their paper, the dispersion relation was derived from the Boltzmann's equation in which the collisional integral was disregarded. Conditions for maximum wave growth were obtained from the dispersion relation and the feasibility of a solid state cyclotron maser was demonstrated.

A major difference between the vacuum cyclotron maser and the solid state cyclotron maser is the effect of collisions in the latter. Collision in solids will be a serious obstacle for the phase bunching needed for coherent readiation. The electrons will remain in orbit for a distance close to the mean free path length λ_z . For example, in InSb near 77°K, λ_z is of the order of 10 - 100 μm .^{3,10} For electron velocity of the order of 10^6 m/sec, the Larmour radius $r_L = v_\perp / \Omega$ and the pitch of the spiral $\lambda_c = 2\pi v_z / \Omega$ are of the order of .1 μm and 1 μm , respectively, for a magnetic field $H_0 \cong 5$ kOe. v_\perp and v_z are, respectively, the components

of electron velocity perpendicular and parallel to the magnetic field. r_L and λ_c are both much smaller than the mean free path and a large number of turns (λ_z/λ_c) of the electron spiral occurs within λ_z . Thus, electron cyclotron maser interaction can take place if the interaction length is of the order of λ_z , but the conditions for cyclotron maser interaction rapidly deteriorate when the interaction length goes much beyond λ_z . In this regard, a solid state cyclotron maser in the cavity configuration is expected to offer a very significant advantage over the waveguide configuration because the cavity configuration requires a much shorter interaction length. The reason is as follows. In the waveguide case, the beam interacts with an electromagnetic wave which grows from the noise or near noise level, while in the cavity case the beam interacts with a large amplitude standing wave which has been built up and stored in the cavity. As a result, the interaction is much stronger in the latter case, or in other words, the required interaction length is much shorter in the cavity than in the waveguide in order for the beam to lose the same amount of energy. This is reflected from the fact that in vacuum cyclotron maser experiments, an oscillator (cavity) is generally shorter than an amplifier (waveguide) by one order of magnitude.

Motivated by the above consideration, here we formulate a detailed solid state cyclotron maser theory in cavity. The formalism and the physical expressions to be derived are considerably different from those of the waveguide structure³ although the basic mechanism is similar. The exact spatial field variation has been incorporated in our calculation and the electron Larmor radius has been kept arbitrary. This allows us to examine interactions at the nonfundamental as well as the fundamental cyclotron frequencies. More im-

portantly, the effect of collisions has also been included in our model. It will be shown that the collisional effect is such a dominant limiting factor in the solid state cyclotron maser that the short interaction length afforded by the cavity structure could be a decisive advantage over the waveguide structure.

In section II we calculate the linear response of an annular electron beam as it interacts with the cavity modes. The dynamics of the electron beam is determined from the Vlasov equation while the collisions are treated with an approximate model. In section III we calculate the electron beam-cavity mode coupling coefficient, beam energy gain and the threshold beam power necessary to sustain oscillations on the basis of a cold beam assumption. We also show the dependence of these quantities on the various parameters such as beam position, beam energy, cavity length and the magnetic field. In section IV we discuss the results from our theory and suggest some experimental configurations to observe the oscillations.

II. MODEL AND FORMULATION

Fig.1 shows the configuration of the electron cyclotron maser system under consideration. An annular beam of electrons is guided by the magnetic field B_0 along helical trajectories inside a circular-crosssection InSb cavity (radius R and length $L < \lambda_z$). The electrons are injected at an angle to the magnetic field such that a major part of their kinetic energy is in the form of transverse gyromotion and the rest in the form of axial motion. The axis of the trajectories is along the cavity (z -axis). The cyclotron orbits may or may not encircle the axis of the cavity, depending on how the beam is formed. In Fig.1 the second type of orbits are shown. We make the following simplifying assumptions to obtain the linear response of the electron beam: (i) the beam is sufficiently weak so that its self electrostatic and magnetic fields are small compared with the cavity fields, (ii) the cavity fields are of first order with respect to the applied magnetic field B_0 and the perturbed electron distribution $f^{(1)}$ caused by these fields is of first order with respect to the initial distribution function f_0 , (iii) the distribution function and the cavity fields are independent of the azimuthal angle θ , and (iv) the electron collision frequency is much smaller than the electron cyclotron frequency.

The cavity modes may be classified as TE or TM modes. Cyclotron maser interaction is much stronger for TE modes than the TM modes.¹ Thus we consider only TE modes and in accordance with assumptions (i) and (iii) restrict our attention to TE_{0nm} modes given by

$$E_{\theta}^{(1)} = E_{\theta 0} J_1(k_n r) \sin k_z z \cos \omega t, \quad (2a)$$

$$B_r^{(1)} = (k_z/\omega) E_{\theta 0} J_1(k_n r) \cos k_z z \sin \omega t, \quad (2b)$$

$$B_z^{(1)} = -(k_n/\omega) E_{\theta 0} J_0(k_n r) \sin k_z z \cos \omega t, \quad (2c)$$

where

$$k_z = m\pi/L, \quad (3a)$$

$$k_n = x_n/R, \quad (3b)$$

x_n being the n -th nonvanishing root of $J_1(x)$ and the wave frequency

$$\omega = (k_z^2 + k_n^2)^{1/2} / \sqrt{\mu\epsilon}. \quad (3c)$$

$J_p(x)$ is the Bessel function of order J_p . μ and ϵ denote, respectively, the permeability and the dielectric constant of the medium. $c = 1/\sqrt{\mu_0\epsilon_0}$ is the velocity of light in vacuum. We assume that $\mu = \mu_0$. The subscript (1) refers to the first order quantities. We use MKS units throughout the paper.

The electron distribution function f is determined by the equation

$$\frac{\partial f}{\partial t} + \frac{\vec{p}}{m} \cdot \nabla f - e \left(\vec{E} + \frac{\vec{p} \times \vec{B}}{m} \right) \cdot \nabla_{\vec{p}} f = \left(\frac{\partial f}{\partial t} \right)_{\text{coll}} \quad (4)$$

where $\left(\frac{\partial f}{\partial t} \right)_{\text{coll}}$ is a collision term whose form will be specified later.

On the basis of the two different time scales assumed [assumption (iv)], we may separate the distribution function f into a slowly varying component f_s representing the collisional relaxation of the zero order distribution function and a fast varying component $f^{(1)}$ representing the perturbation caused by the wave field. A characteristic of the cyclotron maser system is that the cavity structure, rather than the electron medium, determines the properties of the wave (spatial profile and dispersion relation, etc.). Thus, only those electrons which interact resonantly with the wave are of importance while the effects of nonresonant electrons can be neglected. As will be demonstrated in

section III, resonant electrons occupy a very narrow region in the velocity space. Hence the initial distribution function of interest to the problem would be one in which all the electrons fall in the resonant region.

Further it is reasonable to assume that if an electron suffers a collision in its path, it will be scattered off the resonant region and consequently its dynamics will no longer be of interest. Thus we may approximately write f_s as

$$f_s(\vec{r}, \vec{p}, t) = f_0(\vec{r}, \vec{p}) \exp[-\nu(t - t_0)], \quad (5)$$

where t_0 is the time an electron first enters the cavity, $\nu = v_z / \lambda_z$ the collision frequency and $f_0(\vec{r}, \vec{p})$ any function which satisfies the zero order Vlasov equation¹¹ in the absence of collisions. Since the cavity length $L < \lambda_z$, very few collisions occur and the approximate form for f_s in Eq.(5) should be adequate for our purpose.

On linearizing Eq.(4) according to the ordering scheme in assumption (ii), we obtain the following equation for the perturbed distribution function $f^{(1)}$,

$$\begin{aligned} & \left[\frac{\partial}{\partial t} + \frac{\vec{p}}{m^*} \cdot \nabla - \frac{e}{m^*} (\vec{p} \times \vec{B}) \cdot \nabla_{\vec{p}} \right] f^{(1)}(\vec{r}, \vec{p}, t) \\ &= -\nu f^{(1)}(\vec{r}, \vec{p}, t) + e \left[\vec{E}^{(1)}(\vec{r}, t) + \frac{\vec{p} \times \vec{B}^{(1)}(\vec{r}, t)}{m^*} \right] \cdot \nabla_{\vec{p}} f_s(\vec{r}, \vec{p}, t) \end{aligned} \quad (6)$$

where $m^* = \gamma m_0$ with

$$\gamma = \left[1 - (v_{\perp}^2 + v_z^2) / v_g^2 \right]^{-1/2} \quad (7)$$

Note that in Eq.(7), the BGK model¹² of collisions has been assumed. Eq.(6) may be solved by the method of characteristics, namely, by integrating it

along unperturbed trajectories of the electrons. Eq.(6) thus reduces to

$$f^{(1)}(\vec{r}, \vec{p}, t) = e \int_{t_0}^t dt' \exp[v(t'-t)] \left[\vec{E}^{(1)}(\vec{r}', t') + \frac{\vec{p}' \times \vec{B}^{(1)}(\vec{r}', t')}{m^*} \right] \cdot \nabla_{\vec{p}'} f_0(\vec{r}', \vec{p}', t'), \quad (8)$$

where the t' integration is along the unperturbed orbits. The primed quantities \vec{r}' and \vec{p}' are treated as functions of t' while \vec{r} and \vec{p} are, respectively the values of \vec{r}' and \vec{p}' at $t' = t$. The lower limit of the integration t_0 is given by $t_0 = t - z/v_z$, i.e. the time an electron at axial position z and time t first enters the cavity. Substituting Eq.(5) in Eq.(8) and using the relation $t_0 = t - z/v_z$, we obtain

$$f^{(1)}(\vec{r}, \vec{p}, t) = \exp[-z/\lambda_z] \cdot \int_{t-z/v_z}^t dt' e \left[\vec{E}^{(1)}(\vec{r}', t') + \frac{\vec{p}' \times \vec{B}^{(1)}(\vec{r}', t')}{m^*} \right] \cdot \nabla_{\vec{p}'} f_0(\vec{r}', \vec{p}', t'). \quad (9)$$

In the absence of collision $f^{(1)}$ is given by the integral alone on the right-hand side of Eq.(9). Collisions reduce $f^{(1)}$ by the factor $\exp[-z/\lambda_z]$.

The methods for evaluating the integral in Eq.(9) are standard¹¹ and the result may be written in the form

$$f^{(1)} = f_+^{(1)} + f_-^{(1)} \quad (10)$$

where

$$f_+^{(1)} = \text{Im} \left[\frac{e E \theta_0}{2\omega} e^{i(k_z z - \omega t) - z/\lambda_z} \left\{ \left(\omega - \frac{k_z p_z}{m^*} \right) \cdot \frac{\partial f_0}{\partial p_\perp} + \frac{k_z p_\perp}{m^*} \cdot \frac{\partial f_0}{\partial p_z} \right\} \right. \\ \left. + \sum_{S=-\infty}^{+\infty} \sum_{S'=-\infty}^{+\infty} i^{S'-1} \frac{J_{S'}(k_n r) G_{SS'}(k_n r_L) X e^{-iS'(\varphi-\theta)}}{\omega - k_z p_z / m^* - S\Omega} \right], \quad (11)$$

with

$$\Omega = eB_0/m^* = \Omega_0/\gamma, \\ r_L = p_\perp/m_0^* \Omega_0, \\ X = 1 - \exp \left[i(\omega - k_z v_z - S\Omega) z/v_z \right], \\ G_{SS'}(x) = J_{S+S'}(x) dJ_S(x)/dx$$

In Eq.(11), $\text{Im}[A]$ indicates the imaginary part of A . φ and θ are, respectively, the polar angles of the momentum and position vectors. p_\perp and p_z denote the components of momentum, $\vec{p} = m^* \vec{v}$, perpendicular and parallel, respectively to the external magnetic field. $f_-^{(1)}$ is given by equation (11) with ω replaced by $-\omega$. In obtaining equation (11) we have used the following relation¹³

$$e^{is\theta_1} J_s(x_1) = \sum_{s'=-\infty}^{+\infty} J_{s+s'}(x_2) J_{s'}(x_3) e^{is'\theta_2}$$

where x_1, x_2, x_3, θ_1 and θ_2 are related through the triangle shown in Fig.2.

The perturbed azimuthal current $J_\theta^{(1)}$ is given by

$$J_\theta^{(1)} = -e \int f^{(1)} v_\theta d^3p = -e \int_0^\infty p_\perp dp_\perp \int_{-\infty}^{+\infty} dp_z \int_0^{2\pi} d\varphi f^{(1)} v_\perp \sin \varphi \quad (13)$$

where $\hat{\phi} = \phi - \theta$. From Eqs.(10)-(13), we obtain after integration by parts over p_{\perp} and p_z

$$J_{\theta}^{(1)} = J_{\theta+}^{(1)} + J_{\theta-}^{(1)}, \quad (14)$$

where

$$J_{\theta+}^{(1)} = \text{Im} \left[\frac{e^2 E_{\theta}}{4m_o^* \omega} e^{i(k_z z - \omega t) - z/\lambda_z} \sum_{s=-\infty}^{+\infty} \sum_{s'=-\infty}^{+\infty} J_{s'}(k r) \right. \\ \cdot \int_0^{\infty} p_{\perp} dp_{\perp} \int_{-\infty}^{+\infty} dp_z \int_0^{2\pi} d\hat{\phi} f_o i^{s'} \left\{ e^{-i(s'-1)\hat{\phi}} - e^{-i(s'+1)\hat{\phi}} \right\} \\ \cdot \left\{ \frac{G_{ss'}(k r_L) p_{\perp}^2 (\omega^2 - k_z^2 v_g^2) X}{\gamma^3 m_o^* v_g^2 \eta^2} - \frac{(\omega - k_z v_z) X \{ 2G_{ss'}(k r_L) + k r_L G'_{ss'}(k r_L) \}}{\gamma \eta} \right. \\ \left. + \frac{i z (1-X) (\omega^2 - k_z^2 v_g^2 - k_z v_g^2 \eta / v_z) p_{\perp}^2}{\gamma^2 m_o^* v_g^2 p_z \eta} \right\} \Bigg], \quad (15)$$

with $\eta = \omega - k_z v_z - s\Omega$ and $G'_{ss'}(x) = d G_{ss'}(x)/dx$. $J_{\theta-}^{(1)}$ is given by Eq.(15) with ω replaced by $-\omega$.

Equation (14) gives the perturbed current for a general distribution function f_o . In the following we specialize to a particular distribution function which is considered to be the most ideal for cyclotron maser operation.⁹ It is constructed from the constants of motion of the system (in the absence of collision): p_{\perp} , p_z and $L_{\theta} = \gamma m^* v_{\perp} r \sin \hat{\phi} - \frac{e}{2} B_o r^2$. We assume that⁹

$$f_o = k \delta \left(r_L^2 - 2L_{\theta}/eB_o - r_o^2 \right) \frac{\delta(p_{\perp} - p_{\perp}^o) \delta(p_z - p_z^o)}{2\pi p_{\perp}} \quad (16)$$

which represents a cold monoenergetic beam moving along helical trajectories with guiding centers distributed uniformly on a cylinder of radius r_0 . The constant k is determined by the normalization condition

$$\int f_0 2\pi r dr d^3p = N \quad (17)$$

where N is the line density of the electrons (i.e. number of electrons per unit length). Eq.(16) may be rewritten as

$$f_0 = \frac{N \delta(p_z - p_z^0) \delta(p_\perp - p_\perp^0)}{2\pi^2 p_\perp \left\{ (r^2 - r_1^2)(r_2^2 - r^2) \right\}^{1/2}} \left\{ \delta(\hat{\phi} - \hat{\phi}_0) + \delta(\hat{\phi} - \pi + \hat{\phi}_0) \right\} \theta(r - r_1) \theta(r_2 - r) \quad (18)$$

where

$$\hat{\phi}_0 = \sin^{-1} \left[(r^2 + r_L^2 - r_0^2) / 2 r r_L \right] ,$$

$$\theta(x) = \begin{cases} 1 & \text{for } x \geq 0 \\ 0 & \text{for } x < 0 \end{cases} ,$$

$$r_1 = |r_0 - r_L| \text{ and } r_2 = |r_0 + r_L| .$$

The idealized distribution function in Eq.(18) leads to results which can be physically interpreted and provides valuable information for the operation of the solid state gyrotron.

III. BEAM POWER GAIN AND THRESHOLD POWER

The time average power gain for all the electrons in the cavity is given by

$$P = \omega \int_0^{2\pi/\omega} dt \int_0^R dr \int_0^L dz J_\theta^{(1)} E_\theta^{(1)} . \quad (19)$$

We introduce the following notation:

$$\begin{aligned}
 \beta_g &= v_g/c, \\
 \beta_{10} &= p_1^0/\gamma_0 m_0^* c = v_{10}/c, \\
 \beta_{z0} &= p_z^0/\gamma_0 m_0^* c = v_{z0}/c, \\
 \gamma_0 &= [1 - (\beta_{10}^2 + \beta_{z0}^2)]^{-1/2}, \\
 \tau &= L/v_{z0} \\
 \Delta_0 &= \omega^2 \tau^2 - k_z^2 L^2 \beta_g^2 / \beta_z^2, \\
 \Delta &= \omega \tau - k_z L - s \Omega_0 \tau / \gamma_0, \\
 \Delta' &= \omega \tau + k_z L - s \Omega_0 \tau / \gamma_0.
 \end{aligned} \tag{20}$$

τ is the transit time of the electrons in the cavity and $v\tau = L/\lambda_z$. From Eq.(2a), (14), (15), (18), (19) and (20) we have

$$P = \frac{N L e^2 E_0^2}{8 m_0^* \gamma_0 \omega} \sum_{s=-\infty}^{+\infty} (\alpha_{s1} + \alpha_{s2} - \alpha_{s3} - \alpha_{s4}), \tag{21}$$

where

$$\begin{aligned}
 \alpha_{s1} &= - \frac{H_s(k_{nro}, k_{nrL}) \beta_{10}^2}{\Delta \beta_g^2} \left[\Delta_0 \left\{ N(\Delta) + \frac{M(\Delta)}{\Delta} \right\} - \frac{k_z L \Delta \beta_g^2}{\beta_z^2} N(\Delta) \right] \\
 &+ \frac{Q_s(k_{nro}, k_{nrL})}{\Delta} \cdot (\omega \tau - k_z L) \cdot M(\Delta),
 \end{aligned} \tag{22}$$

$$\alpha_{s2} = \frac{H_s(k_{n0}^r, k_{nL}^r) \beta_{10}^2}{\Delta \beta_g^2} \left[\Delta_0 \left\{ N(\Delta') + \frac{M(\Delta')}{\Delta} - \frac{\Gamma}{\Delta} \right\} - \frac{k_z L \Delta \beta_g^2 N(\Delta')}{\beta_z^2} \right] - \frac{Q_s(k_{n0}^r, k_{nL}^r)}{\Delta} \cdot (\omega t - k_z L) \cdot \left\{ M(\Delta') - \Gamma \right\}, \quad (23)$$

with

$$M(x) = [x(1 - e^{-v\tau} \cos x) - v\tau e^{-v\tau} \sin x] / (x^2 + v^2 \tau^2), \quad (24)$$

$$N(x) = \text{Re} \left[\frac{1 - e^{-v\tau} e^{ix}}{(x + iv\tau)^2} + \frac{i e^{-v\tau} e^{ix}}{x + iv\tau} \right], \quad (25)$$

$$\Gamma = 2k_z L (1 - e^{-v\tau}) / (4k_z^2 L^2 + v^2 \tau^2). \quad (26)$$

The quantities α_{s3} and α_{s4} are, respectively, obtained from α_{s1} and α_{s2} with the following replacements

$$\omega \rightarrow -\omega, \Delta \rightarrow -\Delta' \text{ and } \Delta' \rightarrow -\Delta.$$

The functions $H_s(a_0, a_L)$ and $Q_s(a_0, a_L)$ are defined by

$$H_s = J'_s(a_L) I_s(a_0, a_L), \quad (27)$$

$$Q_s = 2H_s(a_0, a_L) + a_L J''_s(a_L) I_s(a_0, a_L) + \frac{1}{2} a_L J'_s(a_L) [I_{s-1}(a_0, a_L) - I_{s+1}(a_0, a_L)], \quad (28)$$

where

$$I_s(a_0, a_L) = -\frac{2}{\pi} \int_{a_1}^{a_2} da J_1(a) a \sin \hat{\varphi} [(a^2 - a_1^2)(a_2^2 - a^2)]^{-1/2} \sum_{s'=-\infty}^{\infty} J_{s+s'}(a_L) J_{s'}(a) \cos s' \left(\frac{\pi}{2} - \hat{\varphi} \right), \quad (29)$$

and

$$a_1 \equiv |a_0 - a_L|, \quad a_2 \equiv |a_0 + a_L| \quad \text{and} \quad \hat{\phi} = \sin^{-1} \left[(a^2 + a_L^2 - a_0^2) / 2a a_L \right].$$

The integral series in Eq.(29) is evaluated in Appendix A and found to be⁹

$$I_s(a_0, a_L) = J_s^2(a_0) J_s'(a_L). \quad (30)$$

Eq.(21) contains a summation over all harmonics of the cyclotron frequency. As we shall see later, radiation is favored at a particular cyclotron frequency near the synchronous condition

$$\omega - k_z v_{z0} - s \Omega_0 / \gamma_0 = 0.$$

Hence in Eq.(21) we keep only one term. We are mostly interested in the fundamental cyclotron frequency. In later calculations parameters are chosen such that $s = 1$ term dominates. In the case $v = 0$, the quantities α assume the form

$$\begin{aligned} \alpha_1 = & -H_s \cdot \left(\beta_{10} / \beta_g \right)^2 \left[\left(\omega^2 \tau^2 - k_z^2 L^2 \beta_g^2 / \beta_z^2 \right) \left\{ 4 \sin^2(\Delta/2) - \Delta \sin \Delta \right\} \right. \\ & \left. + k_z L (\beta_g^2 / \beta_z^2) \Delta \left\{ \Delta \sin \Delta - 2 \sin^2(\Delta/2) \right\} \right] / \Delta^3 \\ & + 2Q_s \cdot (\omega \tau - k_z L) \sin^2(\Delta/2) / \Delta^2, \end{aligned} \quad (31)$$

$$\begin{aligned} \alpha_2 = & H_s \cdot \left(\beta_{10} / \beta_g \right)^2 \left[\left(\omega^2 \tau^2 - k_z^2 L^2 \beta_g^2 / \beta_z^2 \right) \left\{ 2(1 + \Delta/\Delta') \sin^2(\Delta'/2) - \Delta \sin \Delta' \right\} \right. \\ & \left. + k_z L (\beta_g^2 / \beta_z^2) \Delta \left\{ \Delta \sin \Delta' - 2(\Delta/\Delta') \sin^2(\Delta'/2) \right\} \right] / (\Delta^2 \Delta') \\ & - 2Q_s \cdot (\omega \tau - k_z L) \sin^2(\Delta'/2) / (\Delta \Delta'). \end{aligned} \quad (32)$$

The other two quantities α_3 and α_4 are obtained by the replacements

$$\omega \rightarrow -\omega, \Delta \rightarrow -\Delta' \text{ and } \Delta' \rightarrow -\Delta$$

in the expressions for α_1 and α_2 , respectively.

In Eq.(10) $f_+^{(1)}$ and $f_-^{(1)}$ may be regarded as perturbations in the electron distribution function due to the forward and backward travelling waves which make up the standing cavity modes. In eq.(21), the terms α_{s1} and α_{s2} arise from interaction of $f_+^{(1)}$ with the forward and the backward travelling waves. Similarly, α_{s3} and α_{s4} terms are due to the interaction of $f_-^{(1)}$ with the two waves.

In the expression for α 's, the first term (proportional to $H_s \beta_{10}^2$) arise from the transverse motion of the electrons and the second term (proportional to $(\omega^2 - k_z^2 L) Q_s$) is due to wave induced oscillations. The first term is much larger than the second term unless β_{10} is too low. Hence the coupling between the electron beam and the cavity modes is essentially proportional to $H_s(k_{nO}, k_{nL})$. The first term may be positive (beam power gain) or negative (beam power loss) depending on the phase factor Δ . It is shown in Appendix B that E_ϕ , the amplitude of the component of the cavity electric field tangential to the electron cyclotron orbit (see Fig.1) may be written as

$$E_\phi = -A E_{\theta_0} \sum_{s=0}^{+\infty} H_s^{1/2}(k_{nO}, k_{nL}) \cos s \phi,$$

where $A = 1$ for $s = 0$ and $A = 2$ for $s \neq 0$. Thus $E_{\theta_0} H_x^{1/2}$ may be interpreted as the s -th harmonic component of the effective electric field in the direction of the electron velocity and the beam power gain is proportional to H_s .

In the expression for P , the guiding center position r_0 enters through $H_s(k_{n0}, k_{nL})$. Hence P can be maximized by maximizing H_s with respect to r_0 for each combination of n and s . Numerical computation shows that the optimum value of r_0 is $.48R$ for $n = s = 1$. This value of r_0 will be used in later calculations.

The total stored energy (W) in the cavity is given by

$$W = \pi R^2 L \epsilon J_0^2 (k_n R) E_0^2 / 4 \quad (33)$$

Let us define a dimensionless quantity F

$$F = P \tau / W \quad , \quad (34)$$

as the ratio of the total beam energy gain during one transit time to the total stored field energy. From Eqs. (21), (33) and (34), we get

$$F = \omega_p^2 \tau \alpha / 2 \gamma_0 J_0^2 (x_n) \omega \quad (35)$$

where $\omega_p = (N e^2 / \pi R^2 \epsilon m_0^*)^{1/2}$ and $\alpha = (\alpha_1 + \alpha_2 - \alpha_3 - \alpha_4)$.

The quantity F may be positive or negative depending on the value of the phase factor Δ . The beam generates electromagnetic radiation in the range of Δ for which F is negative.

An actual cavity has a finite Q due to dielectric losses or loading or wall resistivity or end-faces not being perfectly reflecting and energy is lost from the cavity at the rate

$$P_{out} = \omega W / Q \quad (36)$$

The electron beam generates energy at the rate

$$P_{in} = -F W / \tau \quad (37)$$

Thus the threshold condition for cavity oscillations is given by

$$-F Q \geq \omega \tau \quad (38)$$

The energy of the electrons in the conduction band of the crystal may be written as

$$W_b = (\gamma_o - 1) m_o^* \beta_g^2 c^2, \quad (39)$$

and the electron beam power inside the crystal is

$$P_b = N(\gamma_o - 1) m_o^* \beta_g^2 c^2 v_{zo}. \quad (40)$$

From Eqs. (35), (38) and (40), we find that

$$P_b \geq P_b^{th}, \quad (41)$$

where the threshold beam power P_b^{th} is given by

$$P_b^{th} = -(\omega R/c)^2 \cdot \left\{ \gamma_o (\gamma_o - 1) \beta_g^2 \beta_{zo} J_o^2(x_n) \right\} \cdot \left\{ 4\pi \epsilon m_o^{*2} c^5 / 2e^2 \right\}. \quad (42)$$

The result for cyclotron maser in vacuum is recovered by setting $\epsilon = \epsilon_o$, $\beta_g = 1$ and $m_o^* = m_e$ in Eq.(42). Since $\beta_g = 4.3 \times 10^{-3}$ and $m_o^* = 0.014 m_e$ in InSb at 77°K, the threshold beam power for the solid state cyclotron maser is many orders of magnitude lower than that of the vacuum case. Numerical examples for F and P_b^{th} are given in the next section.

IV. NUMERICAL RESULTS AND DISCUSSION

The quantity F (eq.35) and the product $Q P_b^{th}$ (eq.42) depend on the parameters s , n , m , R , r_o , λ_z , γ_o , v_{10}/v_{zo} and Ω . For numerical examples we

consider only the fundamental mode numbers, i.e., $s = m = n = 1$. In this case $x_n = k_n R = 3.832$, $k_z L = \pi$ and $\Delta' = \Delta + 2\pi$. As shown earlier r_o should be $.48R$ to maximize $H_s(x_n r_o/R, x_n r_L/R)$. From equations (35) and (42) it can be seen that the radius of the cavity, R , may be scaled out by normalizing length to R and frequency to c/R . Wave vector, time and velocity are correspondingly normalized. The natural dimensionless quantities γ_o , β , Δ , $\omega\tau$, $k_z L$, H_s and Q_s remain unchanged. For a given $\bar{L} = L/R$, $\bar{\omega} = c\omega/R$ is fixed by Eq.(3c). F and $Q P_b^{th}$ are obtained numerically for various values of the parameters \bar{L} , γ_o , β_{1o}/β_{zo} and $\bar{\Omega} = c\Omega/R$ (i.e. Δ).

Figs. 3a and 3b show typical plot of F as a function of Δ .

F becomes negative for Δ in the range $-.9\pi < \Delta < 2\pi$. The lower limit does not change with \bar{L} and shows slight changes only with γ_o , and β_{1o}/β_{zo} . The maximum negative gain, $-F_m$, increases with increase in γ_o , β_{1o}/β_{zo} and \bar{L} . The magnitude of F decreases with $\omega\tau$ as expected. α_1 , α_2 , α_3 and α_4 are also plotted as function of Δ in fig. 3. α_4 differs only slightly from α_2 . In the travelling wave structure, the gain is determined by the term α_1 . In this case gain is negative only^{3,8} for $\Delta > 0$. The phase factor Δ_m corresponding to $-F_m$ lies near $+.1\pi$. Δ_m shifts slightly towards lower values with increase in \bar{L} , γ_o and β_{1o}/β_{zo} .

In Fig.4, $Q P_b^{th}$ is plotted as a function of the electron energy in the crystal $W_b = (\gamma_0 - 1)m_0^* c^2 \beta_g^2$ for cyclotron frequency $\bar{\Omega}$ corresponding to Δ_m . Data are shown for $\beta_{10}/\beta_{z0} = 1.5$ and different values of \bar{L} and $\nu\tau = L/\lambda_z$. The threshold power increases with decrease in \bar{L} and increase in $\nu\tau$. $Q P_b^{th}$ is of the order of 10^{-3} watts for electron energies $\sim 10^{-3}$ ev. For $\bar{L} = .05$ and $\nu\tau = .5$, $Q P_b^{th} = 1.8$ mW at $W_b = 13.2$ m ev. Assuming $Q \approx 100$, $P_b^{th} \approx 18$ μ W. As the length of the cavity is decreased to reduce the effect of collisions, the lowest eigenfrequency increases. For mean free path $\lambda_z \approx 100$ μ m and $\bar{L} = .05$, the operating frequencies at $\nu\tau = 1.0$ and 0.5 are, respectively, 367 GHz and 734 GHz. The corresponding cyclotron frequencies Ω for maximum beam energy loss are 357.4 GHz ($H_0 = 1787$ Oe) and 715 GHz ($H_0 = 3575$ Oe).

We make some suggestions for possible experiments to observe solid-state cyclotron maser radiation. The cavity might be in the form of a disc with polished ends and metallized edges. The thickness of the disc should be less than a mean free path of the electrons. The cavity is placed in a uniform magnetic field. One end-face of the disc is bombarded by an electron beam at an angle to the field such that the electrons get into the conduction band with appropriate transverse and axial velocities. Another possibility is to use the structure under forward bias condition with a doping profile similar to that of a Read diode¹⁴ ($n^+ p i p^+$) such that there is a very narrow accelerating region of high d.c. electric field and a longer intrinsic region where the d.c. electric field is negligible. Cyclotron maser radiation takes place in this region.

V. CONCLUSION

In this paper we propose the operation of a solid-state cyclotron maser in the cavity configuration and demonstrate its feasibility with a theoretical analysis. We have derived analytical expressions for both the electromagnetic power gain and the threshold beam power. The dependence of these two quantities on the various parameters such as the length and radius of the cavity, electron mean free path, the magnetic field, initial electron beam energy, radial and axial eigenmode number, cyclotron mode, etc. has been shown. In order to minimize the effects of collision, the cavity length should be less than a mean free path of electrons. This sets a lower limit to the frequency that can be used. It is seen from Eqs. (35) and (40) that a better performance is obtained with a material having large mean free path λ_z , small band gap i.e. v_g and small effective mass m_o^* . The cavity length can be increased and the frequency of operation lowered if λ_z is larger. Since the cyclotron frequency is proportional to B_o/m_o^* , smaller magnetic fields are required for materials with smaller m_o^* . Furthermore, P_b^{th} decreases as m_o^{*2} . A smaller value of v_g is also desirable because P_b^{th} is lowered and electron velocity needed to obtain a given value of γ_o is also reduced. Our results are based on a linear theory. A nonlinear theory is necessary to calculate the efficiency and the saturation power level of the system. This will be the subject of a future investigation.

The authors are indebted to Dr.K.L.Davis for many helpful discussions.

Appendix A

EVALUATING THE INTEGRAL SERIES $I_s(a_0, a_L)$

The integral series $I_s(a_0, a_L)$ appearing in Eqs. (27) and (28) is defined as

$$I_s(a_0, a_L) \equiv \frac{-2}{\pi} \int_{a_1}^{a_2} da \sin \phi_0 J_1(a) a [(a^2 - a_1^2)(a_2^2 - a^2)]^{-1/2} \cdot \sum_{s'=-\infty}^{\infty} J_{s+s'}(a_L) J_{s'}(a) \cos s' \left[\frac{\pi}{2} - \phi_0 \right], \quad (\text{A.1})$$

where

$$a_1 = |a_0 - a_L|,$$

$$a_2 = a_0 + a_L,$$

and

$$\phi_0 = \sin^{-1} [(a^2 + a_L^2 - a_0^2)/2aa_L] \quad (\text{A.2})$$

Inserting Eq. (A.2) into Eq. (A.1) and using the Bessel function identity

$$J_s(w) \cos s\psi = \sum_{s'=-\infty}^{\infty} J_{s+s'}(u) J_{s'}(v) \cos s'\alpha, \quad (\text{A.3})$$

where $w = (u^2 + v^2 - 2uv \cos \alpha)^{1/2}$ and $\psi = \cos^{-1} [(u - v \cos \alpha)/w]$, we reduce Eq. (A.1) to (after some algebra)

$$I_s(a_0, a_L) = -\frac{J_s(a_0)}{\pi} \int_{a_1}^{a_2} da \frac{J_1(a) (a^2 + a_L^2 - a_0^2)^2}{a_L [(a^2 - a_1^2)(a_2^2 - a^2)]^{1/2}} \cos \left[s \cos^{-1} \frac{a_L^2 + a_0^2 - a^2}{2a_0 a_L} \right]. \quad (\text{A.4})$$

To carry out the integration in Eq. (A.4), we replace the variable of integration a with x , where x is defined through the equation

$$a = (a_0^2 + a_L^2 - 2a_0 a_L \cos x)^{1/2}.$$

Again after some algebra, we obtain

APPENDIX A

$$I_s(a_0, a_L) = -\frac{J_s(a_0)}{\pi} \int_0^\pi dx \frac{J_1[(a_0^2 + a_L^2 - 2a_0a_L \cos x)^{1/2}]}{(a_0^2 + a_L^2 - 2a_0a_L \cos x)^{1/2}} \cdot (a_L - a_0 \cos x) \cos sx$$

$$= \frac{1}{\pi} J_s(a_0) \frac{d}{da_L} \int_0^\pi dx J_0[(a_0^2 + a_L^2 - 2a_0a_L \cos x)^{1/2}] \cos sx, \quad (A.5)$$

Using tabulated integral formula,¹³ we obtain

$$I_s(a_0, a_L) = J_s^2(a_0) J_s'(a_L). \quad (A.6)$$

APPENDIX B

The component of the cavity electric field tangential to the electron cyclotron orbit is

$$\begin{aligned} E_\phi &= E_\theta \cos \alpha \\ &= E_{\theta 0} J_1(k_n r) \cos \alpha, \end{aligned} \quad (B1)$$

where the z -dependence of E_ϕ has been neglected. We may express E_θ in terms of r_0 , r_L , and ϕ through the following geometrical relations (see Fig. 1):

$$\begin{aligned} r &= (r_0^2 + r_L^2 - 2r_0 r_L \cos \phi)^{1/2} \\ \cos \alpha &= [r_L + r_0 \cos(\pi - \phi)]/r \\ &= (r_L - r_0 \cos \phi) / (r_0^2 + r_L^2 - 2r_0 r_L \cos \phi)^{1/2} \end{aligned}$$

Thus,

$$\begin{aligned} E_\phi &= E_{\theta 0} J_1[k_n (r_0^2 + r_L^2 - 2r_0 r_L \cos \phi)^{1/2}] (r_L - r_0 \cos \phi) \\ &\quad \cdot (r_0^2 + r_L^2 - 2r_0 r_L \cos \phi)^{-1/2} \\ &= -E_{\theta 0} k_n^{-1} \frac{\partial}{\partial r_L} J_0[k_n (r_0^2 + r_L^2 - 2r_0 r_L \cos \phi)^{1/2}]. \end{aligned} \quad (B2)$$

Expanding E_ϕ in terms of the sinusoidal harmonics of ϕ and noting that E_ϕ is an even function of ϕ , we obtain

$$E_\phi = \sum_{s=0}^{\infty} E_{\phi s}^s \cos s\phi \quad (B3)$$

APPENDIX B

where

$$E_{eff}^s = \frac{\Theta}{\pi} \int_0^\pi d\phi E_\phi \cos s\phi$$

$$= -\Theta E_{\theta 0}(k_n \pi)^{-1} \frac{\partial}{\partial r_L} \int_0^\pi d\phi J_0[k_n(r_0^2 + r_L^2 - 2r_0 r_L \cos \phi)^{1/2}], \quad (B4)$$

$$\Theta = \begin{cases} 1, & s = 0 \\ 2, & s \neq 0. \end{cases}$$

Using tabulated integral formulae,¹³ we obtain from Eq. (B4),

$$E_{eff}^s = -\Theta E_{\theta 0} J_s(k_n r_0) J_s'(k_n r_L).$$

$$= -\Theta E_{\theta 0} H_s^{1/2}(k_n r_0, k_n r_L) \quad (B5)$$

REFERENCES

- 1 V.A.Flyagin, A.V.Gaponov, M.I.Petelin and V.K.Yulpaten, IEEE Trans. Microwave Theory Tech. 25, 514 (1977) and references therein.
- 2 J.L.Hirshfield and V.L.Granatstein, IEEE Trans.Microwave Theory Tech., 25, 522 (1977) and references therein.
3. A.M. Kalmykov, N.Ya.Kotsarenko and S.V.Koshevaya, Izv.Vyssh.Uchebn. Zavedeniy MV I SSO SSSR po Razdelu Radioelektronika, 18, 93 (1975)
4. E.O.Kane, J.Phys. and Chem.Solids, 1, 249 (1957)
5. J.M.Ziman, "Principles of the Theory of Solids," Cambridge Univ.Press, London, (1964), p.147
6. B.Lax, "Quantum Electronics," Columbia Univ.Press, New York,(1968) p.248
7. H.J.Fossum and B.Ancker-Johnson, Phys.Rev.B8, 2850 (1973)
8. E.Ott and W.M.Manheimer, IEEE Trans.on Plasma Science, PS-3, 1, (1975)
9. K.R.Chu, Naval Research Laboratory Memorandum Report No.3672 (April 1978); Physics of Fluids, 1978 (To be published)
10. J.Gornik, T.Y.Chang, T.J.Bridges, V.T.Nguyen, J.D.McGee and W.Muller, Phys.Rev.Letters, 40, 1151 (1978)
11. D.E.Baldwin, J.B.Bernstein and M.P.H.Weenik, "Kinetic theory of plasma waves in a magnetic field," Advances in Physics (Interscience, New York, 1969), Vol.3, p.1.
12. P.L.Bhatnagar, E.P.Gross and M.Krook, Phys.Rev., 94, 511 (1954)

REFERENCES

13. M.Abramowitz and I.A.Stegun, "Handbook of Mathematical Functions,"
(Dover, New York, 1965), p.363.
14. S.M,Sze, "Physics of Semiconductor Devices," John Wiley & Sons,
New York, 1969, p.200.

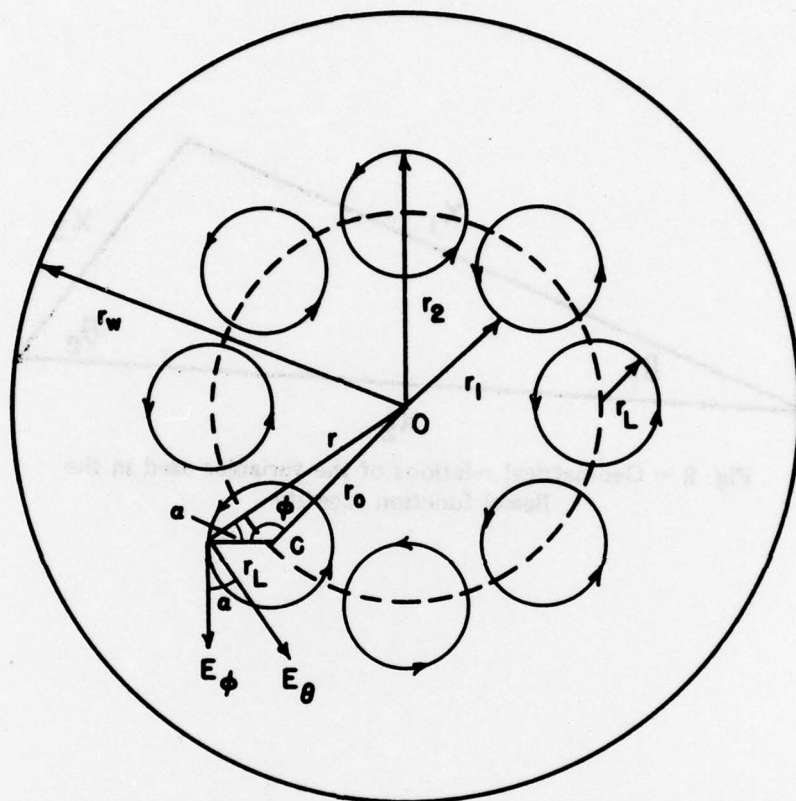


Fig. 1 — End view of the electron cyclotron maser. Guiding centers are uniformly distributed on a circle of radius r_0 . The point O is the axis of symmetry. The circle of radius r_L is an arbitrarily chosen electron orbit and c is the guiding center of this electron. E_θ the electric field of the cavity and E_ϕ the component of E_θ tangential to the electron orbit.

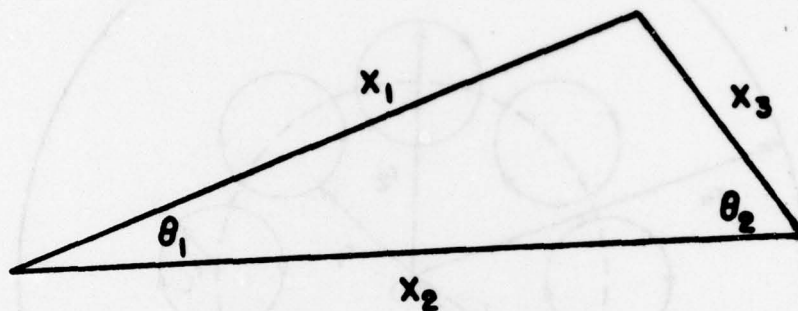


Fig. 2 — Geometrical relations of the variables used in the Bessel function identity

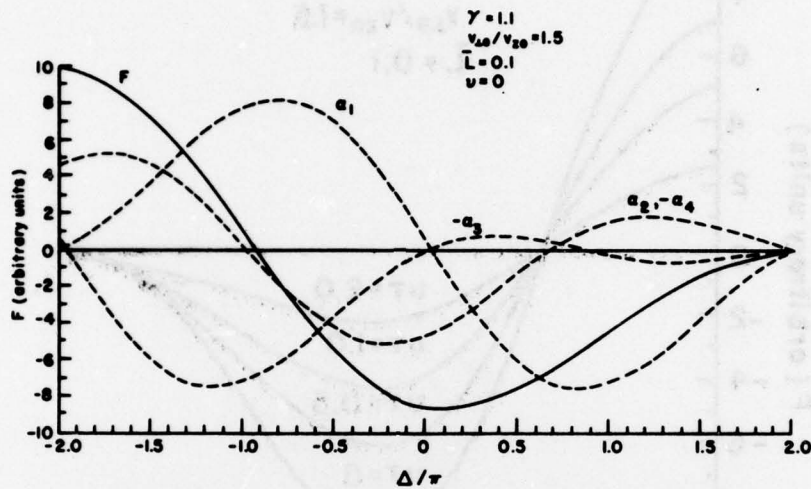


Fig. 3 (a) — F (solid curve) vs. Δ for $n = s = m = 1$, $\bar{r}_0 = 0.48$, $\bar{L} = 0.1$, $\gamma_0 = 1.1$, $\beta_{10}/\beta_{20} = 1.5$ and $\nu\tau = 0$. The dashed curves marked α_1 , α_2 , α_3 and α_4 are plots of the four components of F as function of Δ . Dielectric constant $\epsilon = 17.7 \epsilon_0$.

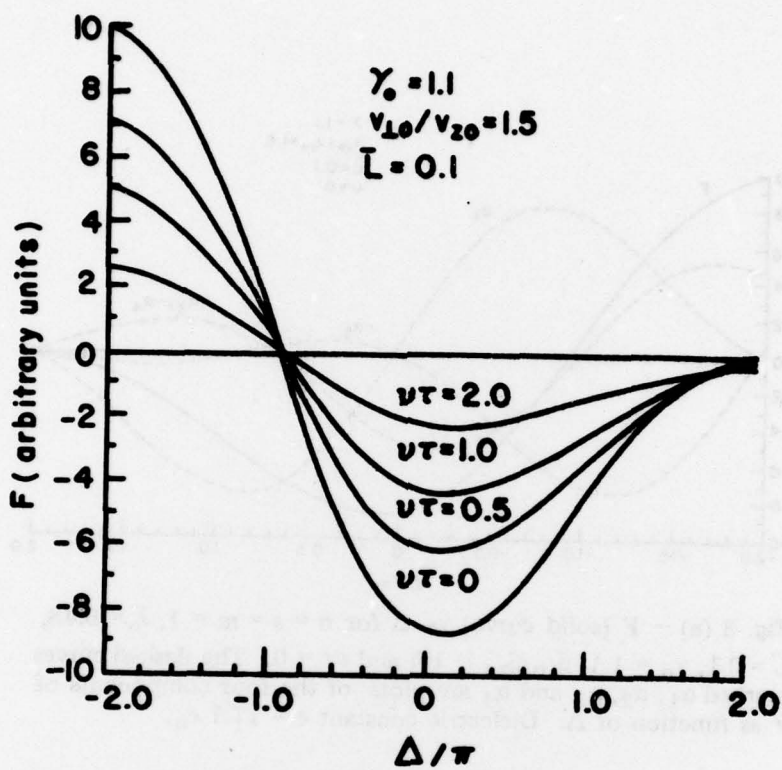


Fig. 3(b) — F as a function of Δ for four different values of $\nu\tau$ with other parameters the same as in Fig. 3(a)

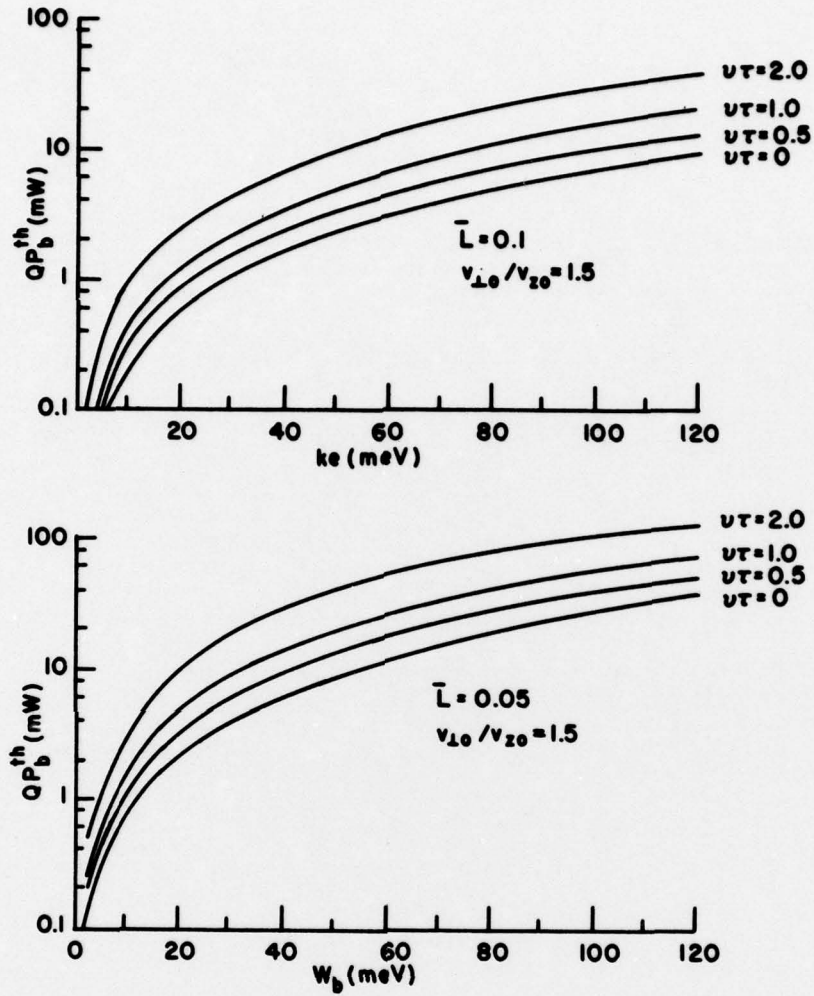


Fig. 4 — P_b^{th} , the threshold beam power, as a function of the beam kinetic energy, W_b , for $n = s = m = 1$, $\bar{r}_0 = 0.48$, $\beta_{\perp 0}/\beta_{z0} = 1.5$ and (a) $\bar{L} = 0.1$, (b) $\bar{L} = 0.05$. The magnetic field is chosen so as to maximize the beam energy loss. Curves are shown for three different values of $\nu\tau$.

79